4th MASHCON, Hamburg - Uliczka et al. (eds) - © 2016 Bundesanstalt für Wasserbau ISBN 978-3-939230-38-0 (Online)
DOI: 10.18451/978-3-939230-38-0_20

PROGRESS ON REAL-TIME PREDICTION OF SHIP-SHIP-SHORE INTERACTIONS BASED ON POTENTIAL FLOW

J A Pinkster, PMH bv, The Netherlands

SUMMARY

A prediction method for ship-ship and ship-shore interaction forces and moment is being developed based on 3-dimensional double-body potential flow. The application of the prediction method is for the purpose of training marine personel on real-time ship manoeuvring simulators for, among others, manoeuvring in ports. To this end a fast accurate prediction method is developed that can be used to model complex port geometries and ship manoeuvres without the penalty of excessive computation times. An existing 3-d flow model is extended to include the option of multi-domains which allows considerably more complex port modelling while keeping the computational load within bounds. To this end the code is run on a desk-top computer fitted with a fast, multi-core GPU which result in a considerable computational speed gain. Examples are given of the application of the multi-domain method. Where appropriate, results of computations are compared with results of the conventional computations which do not make use of the multi-domain option. Finally, an example is given showing that there are realistic cases for which the multi-domain method for computing interactions is probably the only practical option.

1 INTRODUCTION

Ship-ship and ship-shore interactions are part of the disturbances of which the effects on manoeuvring ships in ports are investigated by means of real-time ship simulators. In most simulators ship-ship and ship-shore interactions are included by interpolation of look-up tables of forces and moments on the vessels which have been computed off-line using potential flow methods or, increasingly, CFD methods. Vantorre et al [1] developed empirical models of ship-ship interaction effects for real-time use on manoeuvring simulators based on an extensive set of model tests. In most cases, such interaction forces and moments are treated as external effects acting on the mathematical ship model used in the ship simulator i.e. the interaction model is separate from the mathematical ship model.

The present day trend is to generate ship interactions by computing such effects in real time based on the solution of appropriate hydrodynamic equations taking into account the hull forms of the vessels, the instantaneous position and velocity components of the ships while also taking into account the local port geometry, see [2],[3],[4]. In order for such computations to be useful, the hydrodynamic equations need to be solved sufficiently fast and to deliver sufficiently accurate results on the interaction forces and moments acting on the vessels.

For fast computation of interaction effects of ships in ports the so-called double-body model seems appropriate. The flow is three-dimensional but bounded between the horizontal bottom and equally horizontal mean free surface. The double-body flow model assumes that the speed of the ships is sufficiently low so that the free-surface effect can be neglected. For typical moderate speeds of large ships in ports, it has been shown that the effects of passing ships on large moored vessels are accurately predicted by the computations based on the double-body assumption, see Talstra and Bliek [5]. Until a number of years ago, very few systematic experimental investigations were carried out which could be used to establish the accuracy of predictions of interactions between sailing ships. Results of such investigations, see, for instance [1], are a good basis for evaluation of numerical prediction methods such as the double-body flow method described in this paper.

In its simplest form, the double-body potential flow model predicts interaction effects assuming the ships to be non-lifting bodies. Extensions taking into account lift effects have been investigated in recent years and may find their way into real-time interaction computations in due course. Koning-Gans et al [6]. investigated a double-body potential flow model including lift effects. Bunnik and Toxopeus & Bunnik [7], using a CFD-based code, gave some insight in the effect of the drift angle of the sailing ship on the forces on a moored vessel.

While the quantitative accuracy of the computed interactions between sailing ships is still not well established, it is clear that the most important characteristics of interaction effects seem to be reasonably well predicted even without the inclusion of lift effects. This contribution will be restricted to the non-lifting body version of the double-body flow model.

In order for the computional procedure to be practically useable on a real-time maneuvering simulator, the interaction computations must have a sufficiently fast update rate. An update rate of 2-5 Hz for close maneuvres of overtaking /passing ships seems adequate when there is a high probability of an almost immediate occurrence of a collision. An update rate of 0.3-1 Hz could apply for a vessel carrying out a gentle maneuver such as an approach to a quay or into a lock. There are a number of factors influencing the update rate. The first of these is the complexity of the modelling of ships and port geometry. The more detailed and extensive the modelling, the longer the computation times. Secondly, the sophistica-

tion of the code and the platform used for the computations. Code needs to be optimized and parallelised using all available computing cores of a machine. More computing cores increase the update rate if the code is suitably parallelized.

In a previous paper [4] an approach based on real-time computation of interaction forces using the double-body potential flow model was discussed. The fluid equations were solved based on a Rankine source distribution over zero-order panels describing the wetted surfaces of the vessels and surrounding port geometry. The code is parallelized and the linear equations in the unknown source strengths were solved based on the no-leak condition at the panel centres using a fast Graphical Processing Unit (GPU) which nowadays has up to about 3000 single precision computing cores. All equations were valid for a single fluid domain with constant water depth. In some cases the measured bathymetry of a harbor or channel is used to develop a port panel model. Due to the large number of panels involved special measures have to be taken to retain the necessary update rate for simulator use. It was clear that at the present time GPUs are an affordable means to significantly reduce computation times.

In this contribution this model is extended to include multi-domains i.e. fluid domains each modelling a specific part of the port area with it's own water depth and using features such as symmetry planes to reduce computational load and increase accuracy. By such means a straight vertical quay or a channel with vertical, parallel sides need not be modelled by panels. In this way areas with different water depth are modelled without the necessity to apply panels to the harbor floor. The domains are connected through matching boundaries at which normal velocity and potential are equated in order to assure continuity of the flow conditions through the domains. These matching boundaries involve a limited number of additional panels.

In the following a short introduction is given regarding the double-body flow model and the multi-domain approach.

After the theoretical overview a first example illustrating the accuracy of the matching boundary for the case of forces on a moored vessel due to a passing vessel at a constant water depth will be given. Results of passing vessel forces will be compared for the case with and without a matching boundary around the moored vessel.
A second example illustrates the flexibility in modeling the case of a vessel moored in a so-called pocket, a local increase in water depth to accommodate a deeper draft vessel at lower tide levels. Results will be shown of the forces due to a passing container vessel.
Finally a novel application of the multi-domain concept will be that of a vessel sailing through the matching boundary, for instance, from open water through a narrow channel. Results will be shown which illustrate possibilities and problems with such cases.

2 DOUBLE-BODY POTENTIAL FLOW

The complete model includes the possibility to apply multi-domains. In each domain the theoretical aspects reviewed in the following section apply.

2.1 THEORETICAL BACKGROUND

The computational method is based on 3-d potential theory assuming double-body flow i.e. no free surface deformations and a rigid bottom. The fluid is assumed to be inviscid, incompressible and irrotational. This means that no viscous effects are present in the computed results on forces and moments. The numerical solutions to the flow equations are found based on the boundary element method in which all models, including port geometry are modeled by means of lower order panels.

The vessels are assumed to either lie stationary or sail along an arbitrary track at constant or variable speed in the horizontal plane. The effects of yaw rotations and drift angles are included. Even though the motions of vessels are restricted to three degrees of freedom (surge, sway, yaw), the forces on the vessels are computed for all 6 degrees of freedom.

The numerical model is similar to that described by Korsmeyer et al [8] in that it is based on 3-dimensional potential flow. For the double-body flow model, the potentials describing the flow are based on the Rankine source formulation taking into account restricted water depth and a rigid still water level. To this end the Rankine source formulation needs to be modified to take into account the zero normal velocity which is applicable at both the still water level and the bottom of the waterway. This implies that sources are mirrored an infinite number of times about both the free surface and the bottom. For this code use is made of the formulation given by Grue and Biberg [9]. The infinite mirror series is replaced by a polynomial representation thus making the computations less demanding in terms of time.

2.1 (a) Multi-domain

First the concept of a domain will be clarified. Figure 1 shows docks alongside a channel (A) consisting of three docks B, C and D, each with different water depths with transition slopes between the areas with different water depths.

Shown in the Figure are vessels moored in the docks. The disturbance due to a passing ship propagates into the docks resulting in forces acting on the moored vessels thus generating motions, and forces in mooring lines and fenders.

In conventional double-body flow computations, only one water depth would apply (i.e. the largest water depth), in this case the water depth in the channel (A). The water depth in B, C and D would have to be modelled by a distribution of horizontal panels over the bottom.

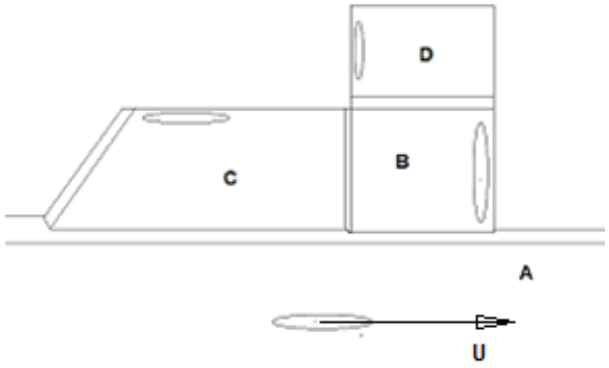

Figure 1. Layout of a port with 4 domains with different water depths.

This could result in a very large number of panels to describe the geometry of the dock and channel adequately. Instead, the port and the sea area are divided in a number of domains, each with their own water depth. That means that when considering the flow within a domain, the potential equations describing the flow would be based on that water depth thus avoiding the necessity of distributing panels over the bottom. Because the domains are separated i.e. sources within a domain have no direct influence on field points in another domain, use can also be made of such features as vertical symmetry planes within each of the domains. A vertical plane of symmetry about which sources on the bodies in the particular domain are reflected creates a perfect reflecting boundary thus avoiding the necessity of panelization of that particular part of the boundary. Symmetry planes are often standard in 3-d codes but only one such construction can be used at a time.

Even though such boundaries stretch infinitely in both directions, their direct influence is now restricted to the particular domain in which they are defined. In this case there are 4 domains i.e. A, B, C and D and each could have a vertical quay section modelled that way. An interesting extension is the ability to make use of double-symmetry planes to model channels with parallel vertical sides, see Newman [10]. In this paper an example is given in which use is made of the double-symmetry approach.

In order to obtain the proper flow in the port and the docks, it must be ensured that the domains are properly connected, i.e. the flow across the boundaries between the domains must be continuous with respect to the momentum flux and mass flow. This is achieved by equalizing the potential and the normal velocities on vertical boundaries between the domains. These vertical boundaries are virtual in that they do not represent physical structures but only serve to ensure the proper flow between the domains. The position of the boundaries is relatively arbitrary but are best chosen so that the other, physical boundaries within a domain can be represented by panels which do not extend below the water depth of that domain. An example is shown in Figure 2 with the location of the boundaries between domain A and domain B as well as between domain B and domain D. This shows that, for instance, the slope between B and D is modelled by panels in domain B. Likewise, the slope between A and B is modelled by panels in A.

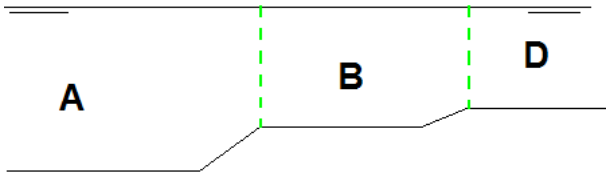

Figure 2. Location of matching boundaries between domains.

How are these boundaries modelled? At these 'matching boundaries', or interfaces between the domains, conditions of equal potential and normal velocity are to be imposed. This is made possible by modelling the interfaces by panels of identical number and size on both sides of the interface. The panels of the interfaces between domains are in a back-to-back situation with positive normal of the two parts of the matching boundary directed into each domain. In the computations the normal velocities and potential at the colocation points of the matching boundary panels belonging to a domain are determined using only the sources within the same domain. Likewise, the normal velocities and pressures on the corresponding panels of the matching boundary belonging to the adjacent domain are computed based on sources in that adjacent domain. An example involving 4 different domains is shown in Figure 3 in which the matching boundaries or interfaces are the checkered parts. The checkering is due to the fact that these panels are in the same location with different normal directions. The hidden surface algorithm gets confused! In the following the equations on the basis of which the flow through the domains and the forces on the moored vessels will be solved, will be discussed.

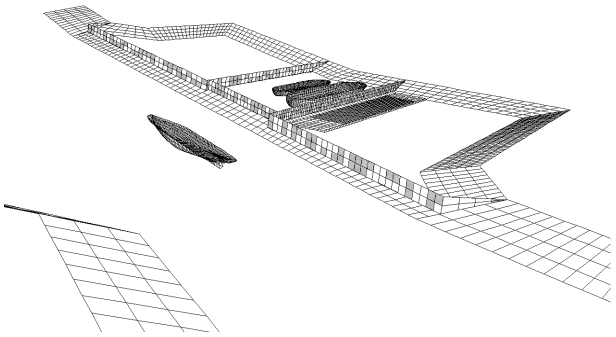

Figure 3. Matching boundaries in a complex port geometry.

The system of equations is arranged so that the port geometry may be subdivided into a number of interconnected domains with in each domain zero or one or more moored vessels.

Assume a passing vessel in the first domain. This means that vessels not moored in the first domain will not 'feel' the disturbance due to te passing vessel directly, but in an indirect manner due to the flow through the interfaces between the domains into the domain in which the particular vessel is moored.

The hydrodynamic equations for the flow within a domain containing moored vessels are given below.

The additional equations for the boundary conditions between the domains are then given. Together equations for the no-leak conditions on each domain (excluding the interfaces) and for all vessels combined with the boundary conditions at the interfaces (equal pressure on both sides and continuity of normal velocity) lead to a set of linear equations in the unknown source strengths which are solved using standard methods.

2.1 (b) Flow equations

The 3-d panel method involves a homogeneously distributed Rankine source on each zero-order panel describing both the ships, port geometry and matching boundaries between domains. Within each domain the potential function ϕ which is dependent on the earth-bound coordinates X,Y,Z and time t containing all information on the flow is the sum of the potentials due only to sources in that domain. At each time step the unknown source strengths are solved based on the no-leak boundary condition at the center of each panel of fixed port structures and sailing vessels in that domain and the boundary conditions valid for the matching boundaries connecting the flow to other domains.

The no-leak condition on panels describing the vessels and panels of fixed port structures may be formulated in terms of the velocity component normal to the target panel as follows:

$$\frac{\partial \phi}{\partial n} = V_n \tag{1}$$

in which:

$$V_n = 0 \tag{2}$$

for fixed port structures and:

$$V_n = (\overline{U} + \overline{r} \times \overline{x}) \cdot \overline{n} \tag{3}$$

for a vessel sailing at speed $\overline{U}$ and rate of yaw rotation $\overline{r}$. The location of a point of the hull is $\overline{x}$ relative to the vessel axes and the normal vector to the hull is $\overline{n}$. The positive normal direction is pointing out of the body into the fluid.

In order to assure the correct transfer of fluid impuls between domains the boundary conditions at the matching boundary between two domains require the normal velocity on both sides of the boundary to be continuous and the potential to be equal. This is achieved by modelling a matching boundary by two identical sets of source panels, one set for each of the two sides of the boundary. The panels are arranged in a back-to-back situation i.e. the side of the matching boundary belonging to a domain has the positive normal direction into the fluid of that domain, see Figure 4.

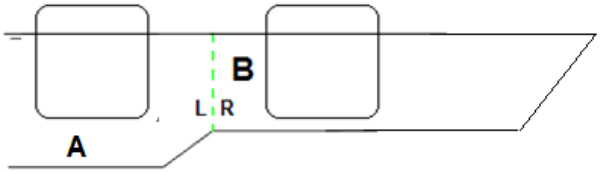

Figure 4. Left and right side of a matching boundary

For the normal velocity at a matching boundary the following requirement applies for each pair of back-to-back panels:

$$\frac{\partial \phi}{\partial n_L} = -\frac{\partial \phi}{\partial n_R} \tag{4}$$

or:

$$\frac{\partial \phi}{\partial n_L} + \frac{\partial \phi}{\partial n_R} = 0 \tag{5}$$

For the potential the following applies:

$$\phi_L - \phi_R = 0 \tag{6}$$

The last two equations require that the normal velocity and potential with index *Left* or *Right* be evaluated based on the sources in the relevant domain.

For the panels on ships and fixed port structures, excluding matching boundaries, the no-leak condition of Equation 1 is applied. For panels on the matching boundaries Equation 5 and Equation 6 are applied.

The number of unknown source strengths is equal to the total sum of panels in all domains including panels on ships, port structures and matching boundaries. The number of linear equations which have to be solved at each time step is equal to the number of unknowns. A large number of influence functions relating a source to a field point will be zero. This will be the case for all combinations where the source is not in the same domain as the field point.

Based on the solutions for the source strengths, the forces and moments acting on the vessels can be computed. The reader is referred to Pinkster [11] for further details of the method of solution of the unknown source strengths when applying matching boundaries in 3-d diffraction computations.

2.1 (c) Hydrodynamic forces

Forces are determined based on the following equation assuming the unit normal $\overline{n}$ pointing out of the body into the fluid:

$$\overline{F} = -\iint_S p\overline{n}dS \tag{7}$$

The pressure p follows from Bernoulli's equation in which the potential ϕ and it derivatives are given relative to an earth-fixed system of axes:

$$p = -\rho\frac{\partial\phi}{\partial t} - \tfrac{1}{2}\rho|\overline{\nabla}\phi|^2 \tag{8}$$

The first term on the right-hand side of this equation is the instationary pressure component including added mass effects. The second term is the pressure drop due to the square of the fluid velocity sometimes referred to as the Bernoulli pressure term. The potential contains contributions from all vessels or bodies, moving or otherwise, in the fluid domains.

In the code the equations for the interaction forces between ships as derived by Xiang & Faltinsen [12] have been implemented. The equations apply to deep or shallow water and take into account arbitrary motions of the vessels.

3 APPLICATION OF DOMAINS

In the following some examples will be given of the application of the domain concept to ship interaction problems. The following cases will be treated:

- Forces on a moored vessel due to a passing vessel
- Passing vessel forces on a tanker moored in a pocket
- Forces on a vessel entering and passing through a narrow channel or lock

In the first and third cases the forces on the vessel will be computed for two cases i.e. using the conventional approach based on a single water depth without and with application of the domain approach. Comparison of the results are intended to illustrate that the results are essentially the same which will indicate that the flow between the domains is modelled correctly.

The second case is added to illustrate the flexibility of the domain approach to analyse unusual cases which cannot be modelled easily otherwise.

In the examples two different ship models are used, a container vessel and a tanker. The main particulars of the vessels are given in Table 1.

Table 1. Main particulars of the vessel

		Container	Tanker
L_{pp}	m	230.0	257.0
Beam	m	32.2	36.8
Draft	m	10.8	15.7
Displacement	m^3	52030	118800
No. of panels	-	828	792

3.1 FORCES ON A MOORED VESSEL DUE TO A PASSING VESSEL

The layout for the conventional case and the case with application of two domains is shown in Figure 5 and Figure 6. The symmetry boundary modelling the vertical quay wall is coloured light blue withing the domain of the moored vessel and grey outside. This is to denote that both parts of the symmetry boundary are declared separately for each domain. In this case they are declared in the same plane to form a continuous, straight vertical quay.

The same container vessel is used both as the moored vessel and the passing vessel, see Table 1. This is a container vessel with a displacement of 52030 m^3. The passing speed is 8 kn and the passing distance is 100 m measured from centreline to centreline. The water depth amounted to 15 m. The moored container vessel centreline is 20 m from the vertical quay.

A rectangular matching boundary measuring 400 m along the vertical quay at a distance of 50 m from the quay was modelled as shown in Figure 6. The location of the matching boundary is relatively arbitrary but is also used in the second example in which the effect of a pocket is included.

The inner and outer vertical matching boundaries are each modelled by 100 panels. These are arranged in two sides perpendicular to the quay at distances of +200 m and -200 m from midship of the moored tanker and one side parallel to and 50 m from the quay.

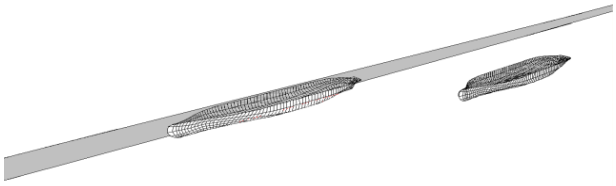

Figure 5. A vessel moored against a vertical quay and a passing vessel.

The panels on the matching boundary are relatively large. This is possible because the flow gradients are relatively low some distance away from the passing or moored ship.

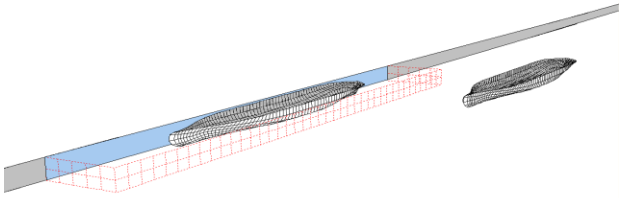

Figure 6. A vessel moored against a vertical quay in a domain surrounded by a matching boundary (red dotted line) and a passing vessel in a second domain.

The computed surge force, sway force and yaw moment on the moored container vessel are shown in Figure 7 for both cases. The results are shown to be almost identical confirming that the matching boundary between the vessels is fully transparent.

In this example the waterdepth in both domains was the same so that the effectiveness of the matching boundary could be established.

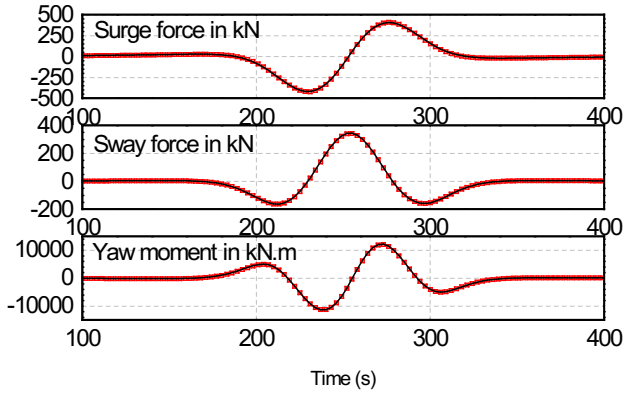

Figure 7. Forces and yaw moment on the moored vessel. Results with application of domains in red. Other results in black. . Surge force positive forward, Sway force positive to port, Yaw moment positive, bow to port.

3.2 PASSING EFFECTS ON A VESSEL MOORED IN A POCKET

An extension to the aforegoing example is to apply the domain split to the case of a tanker moored in a pocket with a greater waterdepth than in the channel through which the passing vessel is sailing. The layout of the matching boundary is the same as in the first case except that a pocket is modelled in the domain around the moored vessel. The water depth in the pocket amounted to 20.0 m while the water depth outside the pocket amounted to 15.0 m. The layout is shown in Figure 8.

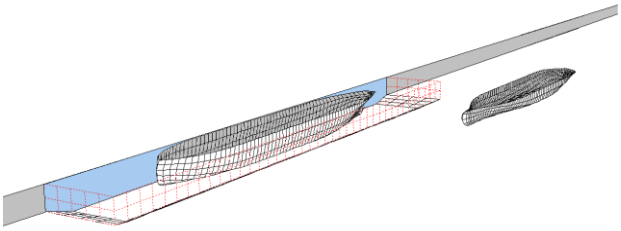

Figure 8. A tanker moored in a pocket surrounded by a matching boundary.

Figure 8 shows the matching boundary (dotted red lines) around the pocket and the pocket side which are modelled as a slope between the water depths of 20 m and 15 m. In this case the moored vessel is a tanker of 118800 m^3 displacement. The passing vessel is again the container vessel. Dimensions of both vessels are given in Table 1. The passing speed is 8 kn and the passing distance between the centrelines of the vessels is 100 m. The moored vessel centreline is 20 m from the vertical quay. The results of the computations are shown in Figure 9.

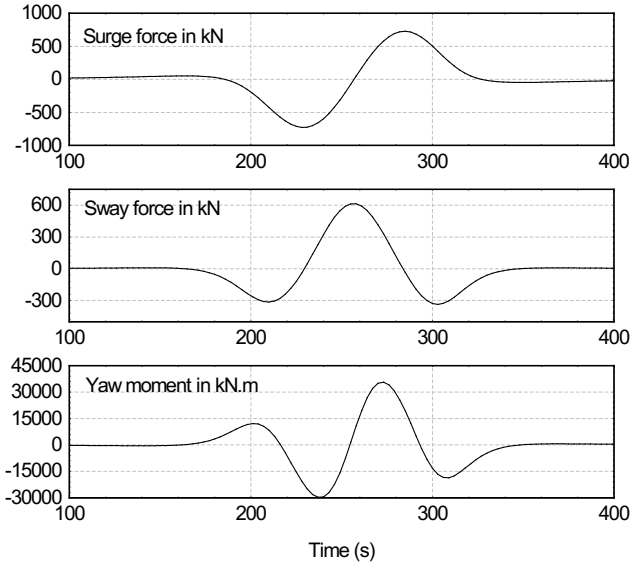

Figure 9. Passing vessel forces on a tanker moored in a pocket.

The overall characteristics of the forces and moment on the moored tanker are similar to the case of a vessel moored to a vertical quay and with the same waterdepth as the channel in which the passing vessel is sailing as shown in Figure 7. The forces and moment are however, generally higher for this case since the moored vessel is larger. A large part of the increased interaction force is related to the gradients of the pressure field generated by the passing vessel acting on the larger volume of the moored vessel.

As the passing vessel closes in on the moored vessel, the surge force on the moored vessel draws the vessel backwards. This reverses to a forward-directed force when the passing vessel passes the midship of the moored vessel.

The peak in the lateral force on the moored vessel is reached when the vessels are abreast and is directed to port, towards the passing vessel.

The yaw moment is positive (bow to port) early in the manoeuvre then changes sign when the bow of the passing vessel is level with the stern of the moored vessel, tending to draw bow and stern towards each other.

This trend reverses as the passing vessel sails past the midship of the moored vessel.

For this case no comparison is made with another method since this is not a case which can be easily modelled using a single water depth. Modelling this layout would require the basic water depth to be equal to the 20.0m water depth in the pocket and the area with a water depth of 15.0 m would need to be modelled with a very large number of horizontal panels.

3.3 FORCES ON A TANKER SAILING THROUGH A NARROW CHANNEL

The last case is that of a vessel entering a 500m long narrow channel (or open lock) with a width of 60m from open water leading to the exit also into open water. The water depth in the open water parts and the channel were equal to 20m.

For this case the focus is on the forces on the sailing vessel. Navigation through restricted channels presents special problems for the vessel since transient forces associated with entering a channel of restricted width and bank suction effects become important. Also the dynamic properties of the vessel are affected by the waterway restrictions. For this reason attention is also paid to added mass effects during the channel transit.

The computations were carried for two cases i.e. for the first case the channel is modelled using panels for the vertical sides and a single domain not requiring matching boundaries.

For the second case use is made of three domains. The first open area is the first domain which is modelled by panels representing vertical quays to either side of the channel entrance. This domain is connected to the second domain, the channel by a matching boundary. At the exit side the channel domain is connected to the domain of the open area by a second matching boundary. A plan view of the vessel entering the narrow channel from open water is shown in Figure 10.

Figure 10 shows the vessel, which is the same tanker used in the last example, entering the channel from open water. The black lines represent the vertical quays at almost right-angles to the channel centreline at the entrance and the exit and also the vertical sides of the 500m long and 60m wide waterway.

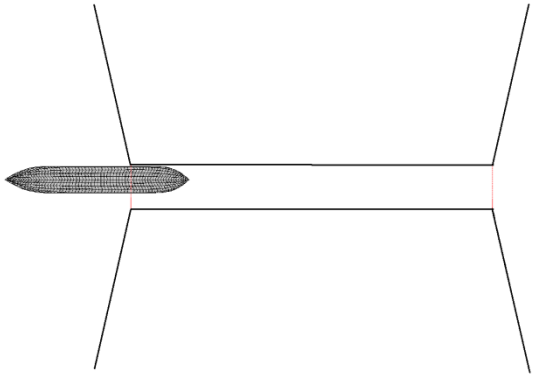

Figure 10. Plan view of a tanker entering a narrow channel from open water.

The vessel is shown 10.0m off-centre of the channel centreline. The beam of the vessel is 36.6 m. This means that the clearance between the port side of the vessel and the quay amounted to 1.7 m. This is an extremely small clearance associated more with a vessel entering a lock than traversing a channel. It is however, important to investigate the robustness of the computational procedure for such extreme cases.

For the computations the vessel speed was set at a constant value of 1 m/s. The track was parallel to the channel axis.

The panel model used to compute the forces on the vessel without making use of the domain concept is shown in Figure 11.

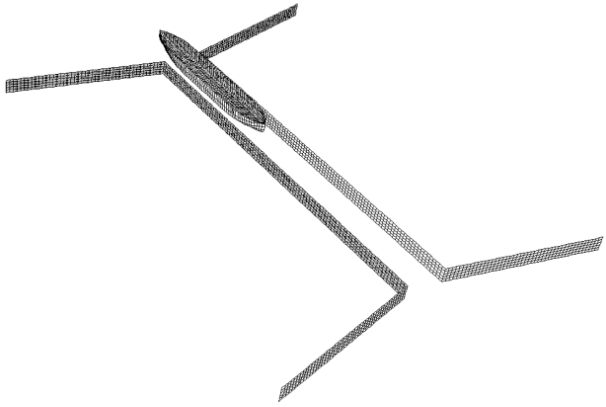

Figure 11. Channel sides modelled by panels.

The total number of panels used to model the channel amounted to 1900, of which 1000 panels were devoted to the 500 m long parallel quays.

The corresponding model developed using three connected domains is shown in Figure 12 and in Figure 13.

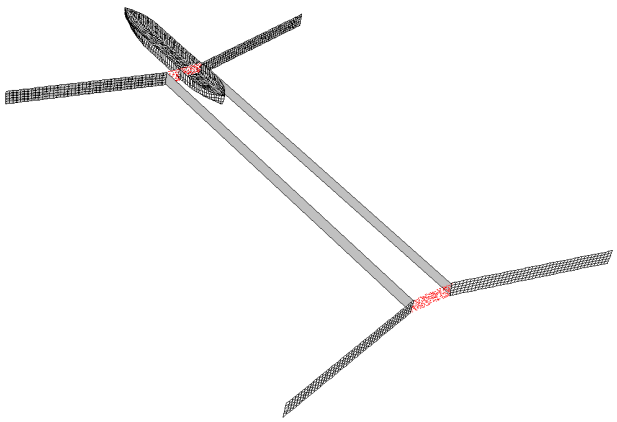

Figure 12. Channel sides modelled by double-symmetry. Matching boundaries at entrance and exit to the channel.

In Figure 12 and Figure 13 the channel sides are shown as a single grey panel. This represents the double-symmetry boundaries about which the potentials are mirrored in order to achieve the no-leak condition for all points of the channel sides. The matching boundaries at the channel entrance and exit are shown in red dots. Each matching boundary is modelled with 330 panels. The total number of additional panels for the matching boundaries amounted to 4 x 330 = 1320 which is 120 more than used for the model shown in Figure 11.

A detail of the intersection of the vessel with the matching boundary is shown in Figure 13. In Figure 13 it is seen that the matching boundary extends through the vessel model. No modifications are made to the matching boundary at any point.

The vessel panel model is cut at the intersection between vessel and matching boundary.

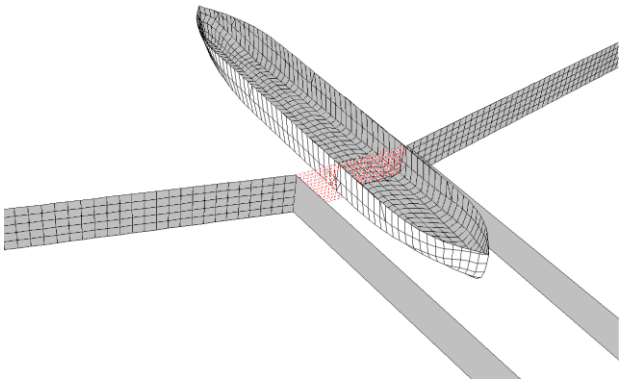

Figure 13. Detail of the matching boundary at the channel entrance and the intersection with the panel model of the ship.

Panels which are cut by the matching boundary are re-modelled into parts which are in one of the two domains on either side of the matching boundary depending on the location of the collocation point of the panel sections relative to the matching boundary.

This approach means that at each step the panel model of the vessel is modified in the vicinity of the matching boundary. It may be that a vessel is crossing more than one matching boundary at the same time. This is also taken into account in the computational procedure.

The results of the computations for this case are shown in Figure 14 through Figure 16.

The vessel starts with the midship located 300 m from the channel entrance. As can be seen, the added mass values start to rise and when the vessel is completely in the channel are about double the open water values. As the vessel leaves the channel values drop back down to the open water levels. Higher added mass values indicate that it will be more difficult to change a manoeuvre in the channel than outside of it.

The results in the figures show that when the vessel is completely in the channel, the difference between the methods amounts to 15-20% for the surge added mass. Predictions for the sway and yaw added mass values are almost the same for both methods.

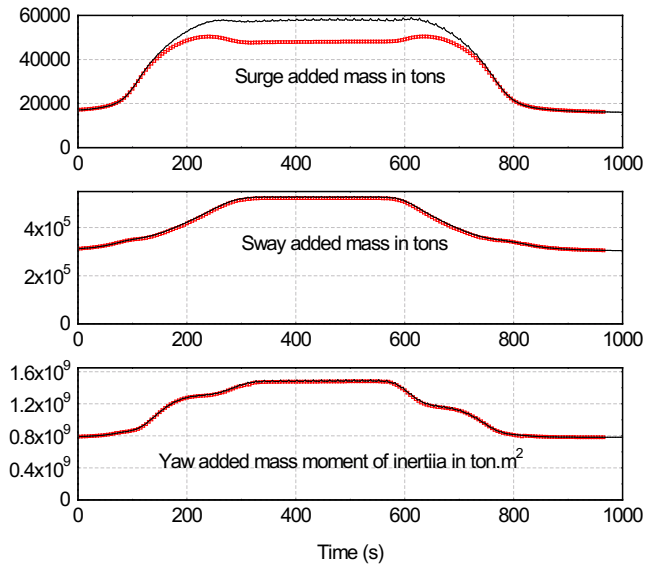

Figure 14. Added mass of the vessel. Domain results in red. Panel model results in black.

Another important component of the forces on the vessel are those due to the fluid pressure drop which occurs when the fluid velocity increases. This is the second term in Equation 8, sometimes referred to as the Bernoulli term. Results of computations of these force components are shown in Figure 15.

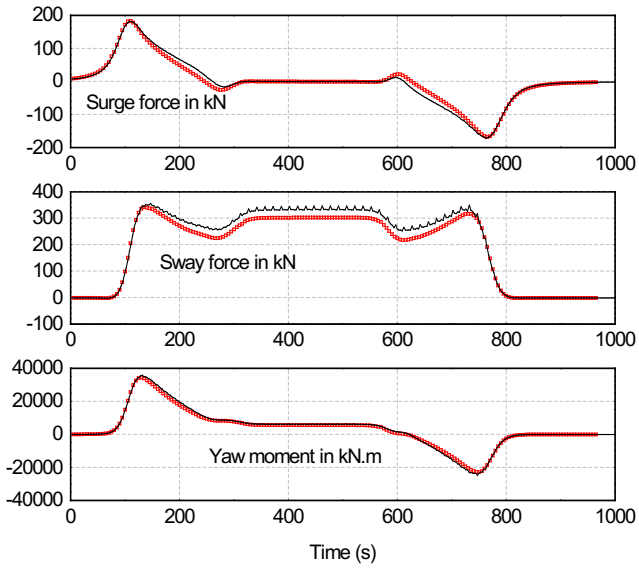

Figure 15. Bernoulli pressure term contribution to the forces and yaw moment on the vessel. Domain results in red. Panel model results in black. Surge force positive forward, Sway force positive to port, Yaw moment positive, bow to port.

Results shown in Figure 15 for this component of the surge force indicates that as the vessel approaches and enters the channel a forward-directed force is generated sucking, as it were, the vessel into the channel. When the vessel is in the channel the surge force drops to zero. This in keeping with, or in line with double-body potential flow theory. Since there is no viscosity, no shear forces are generated and no flow separation occurs leading to zero longitudinal force under constant conditions i.e. without significant effects from the channel entrance or exit. As the vessel exits the channel a resistance increase occurs tending to slow the vessel down in this phase. It should be remembered that this term is one of the two main force components arising from Equation 8.

The transverse force shown in Figure 15 indicates a force value which rises to about 300 kN when the vessel has fully entered the channel. Some variations are shown entering and exiting the channel. The transverse force is directed to port (positive value) as can be expected from the bank suction phenomenon.

The yaw moment acting on the vessel as it enters the channel is directed bow to port. As the vessel proceeds into the channel the port-directed moment decreases but stays at a non-zero positive value for most of the time. As the vessel approaches the exit the yaw moment becomes directed to starboard and drops back to zero when the vessel has cleared the channel. The behaviour of the yaw moment is in keeping with a bank suction force to port on, at first, the bow, and finally the stern.

The overall comparison between the results of both computational methods agree quite well with the domain method results being slightly lower for the sway force when the vessel is fully in the channel.

Finally, the total surge force, sway force and yaw moment on the vessel are examined. The total forces include inertia related terms arising from the pressure Equation 8. The total forces and yaw moment are shown in Figure 16.

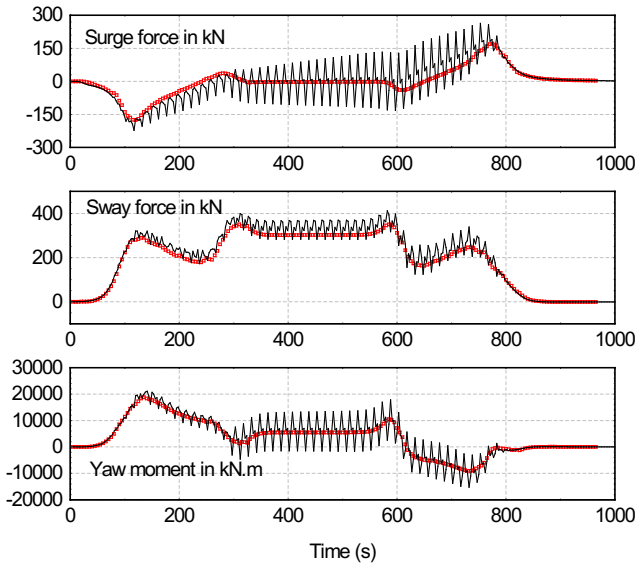

Figure 16. Total forces and yaw moment. Domain results in red. Panel model results in black.

In Figure 16 the differences in the results of the computed forces and yaw moment are quite remarkable. The results based on application of the panel modelling of the channel (solid black line) show distinct spikes. The results found by application of the domain approach combined with the double-symmetry modelling of the channel are, in contrast, quite regular and smooth throughout the simulation.

It is noted that the total surge forces shown in Figure 16 is different from the component of the Bernoulli pressure term shown in Figure 15. At the entrance of the channel the total surge force shows a resistance increase while the Bernoulli term predicts a resistance reduction. The difference is due to the unsteady (first) term in the pressure of Equation 8. This term is related to the rate of change of the surge added mass on approaching the channel entrance. The increasing added mass reflects the kinetic energy in the fluid being increased by the vessel. The reaction to this is the increase in resistance. This increase is sufficient to overcome the negative resistance due to the Bernoulli term.

On average, both methods of computation of the hydrodynamic forces agree reasonably well however, in a real time application of forces with strong fluctuations to a dynamic simulation of ship manoeuvres may lead to unstable simulation results and are as such undesirable.
The cause for the fluctuations in the forces and yaw moment are related to the fact that the source panels on the

vessel are sliding past the source panels of the channel sides. This results in what might be termed a 'cobblestone effect' in the results. This can only be reduced effectively by increasing the number of panels on both the vessel and the channel sides. This is, however, detrimental with respect to the computation effort and is also undesirable. Slight fluctuations are also seen in the added mass terms in Figure 14 and the Bernoulli pressure force terms shown in Figure 15 for the method using panels on the channel sides. These effects magnified in the total forces since the inertia term contribution, which is related to the added mass terms, is based on differentiation with respect to time.

Due to the fact that in the domain approach no panels are used to model the channel sides, the cobblestone effect is absent.

The results show that the multi-domain approach, which makes it possible to apply the double-symmetry model to the channel while leaving the entrance and exit to the channel open, is an attractive alternative. All the more so since it also allows water depth differences between the domains to be easily modelled as well.

4 CONCLUSIONS

In this paper multi-domain method for the prediction of ship-ship interactions based on the double-body potential flow equations was introduced. Comparative computations were carried with the domain method and the conventional method based on constant waterdepth and using only panels to model port geometry. Results show that for the classic case of passing vessel effects on a ship moored alongside a vertical quay, the predictions for forces on the moored vessel are almost identical.
The domain method was subsequently applied to the case of a vessel moored in a pocket alongside a vertical quay for which the conventional method is less suitable due to the extreme large number of panels needed to model the channel floor outside the pocket.

Finally, comparative computations were carried out for the case of a tanker sailing off-centre through a narrow channel. Results of added mass agreed reasonably well as well as the force components based on the velocity-dependent part of the pressure (Bernoulli pressure term). It was shown that, for a vessel passing closely to a vertical quay in the narrow channel, the conventional method based on modelling the channel sides by means of panels, extreme spikes appeared in the force records due to a 'cobblestone' effect related to the proximity of the panels of ship and channel.

Due to the use of the double-symmetry option to model the channel, this cobblestone effect is not present in the domain method.

There are some aspects which have not been addressed in this paper:

- Computation times have not been discussed. At this stage of the development the most important aspects are the accuracy and consistency of the results. Computations are carried using a GPU to speed up computations but the code has not been fully optimized.
- Potential flow computations of passing ship effects on moored ships have been correlated with model test results and found to be reliable for typical harbour speeds of large ships. [4]. For the ship-ship interaction problem, few comparisons have been made between computed and experimental results. This will be part of the future effort with respect to the development and the evaluation of the present method.

5 REFERENCES

1. Vantorre, M.; Verzhbitskaya, E.; Laforce, E. (2002). Model Test Based Formulations fo Ship-Ship Interaction Forces. *Ship Technology Research* Vol. 49, pp 124-141.

2. Sutulo, S; Guedes Soares, C.; Otzen, J.F. (2012). Validation of Potential-Flow Estimation of Interaction Forces Acting upon Ship Hulls in Parallel Motion*, Journal of Ship Research*, Vol.56, No.3, pp 139-145. SNAME

3. Lindberg, O.; Bingham, H.B.; Engsig-Karup, A.P.; Madsen, P.A. (2012). Towards Realtime Simulation of Ship-Ship Interaction*. 27th International. Workshop on Water Waves and Floating Bodies*. Kopenhagen.

4. Pinkster, J.A.; Bhawsinka, K. (2013). A real-time simulation technique for ship-ship and ship-port interactions. *28th International Workshop on Water Waves and Floating Bodies*. L'Isle sur la Sorgue, France

5. Talstra, H; Bliek, A.J. (2014). Loads on moored ships due to passing ships in a straight harbor channel. *PIANC World Congress*, San Francisco.

6. Koning Gans, H. J. de; Huijsmans, R.H.M.; Pinkster, J.A. (2007). A Method to Predict Forces on Passing Ships under Drift. *9th International Conference on Numerical Ship Hydrodynamics*, Ann Arbor, Michigan.

7. Bunnik, T.; Toxopeus, S. (2011). On the modeling ofpassing ship effects, *26th International Workshop onWater Waves and Floating Bodies,* (IWWWFB 2011),Greece.

8. Korsmeyer, F.T.; Lee, C.-H.; Newman, J.N. (1993). Computation of Ship Interaction Forces in RestrictedWaters, *Journal of Ship Research*, Vol. 37, No. 4, pp 298-306

9. Grue, J.; Biberg, D. (1993). Wave Forces on MarineStructures with small speed in water of restricted depth, *Applied Ocean Research* 15, pp 121-135

10. Newman, J.N. (1992). The Green function for potentialflow in a rectangular channel. *Journal of Engineering Mathematics* 26: 51-59

11. Pinkster, J.A. (2011). A multi-domain approach in 3-d diffraction calculations. *30th International Conference on Ocean, Offshore and Arctic Engineering*, Rotterdam.

12. Xiang, X.; Faltinsen,O.M. (2010). Maneuvering of Two Interacting Ships in Calm Water, *11th International Symposium on Practical Design of Ships and Other Floating Structures*, Rio de Janeiro.

6 AUTHOR'S BIOGRAPHY

J. A. Pinkster is a graduate of Delft University of Technology and he obtained a PhD from the same university in 1980. He worked at MARIN, Wageningen from 1970-1990 and subsequently became Professor of Ship Hydromechanics in the Marine Technology Department of Delft University. He retired from Delft in 2006 and has since then been active in consultancy for the marine community and in the development of new methods of analysis for ships and offshore structures.